

or, changing variables, $\cosh x = \gamma\gamma'(1 + \beta\beta' \cos\theta^*)$:

$$\frac{a_l^\Lambda}{a_l^\Sigma} = \int \frac{\sinh x \, dx}{\gamma\gamma'\beta\beta'} P_l \left(\frac{\cosh x - \gamma'/\gamma}{\beta \sinh x} \right). \quad (\text{A4b})$$

The coefficients are evaluated for $l=0-4$.

$P_0=1$:

$$\frac{a_0^\Lambda}{a_0^\Sigma} = \frac{1}{2} \int_{\theta_1}^{\theta_2} \cos\theta \, d\theta = \frac{1}{2}$$

for the cut actually used, $-1 < \theta^* < 0$.

$P_1 = \cos\theta^*$:

$$\frac{a_1^\Lambda}{a_1^\Sigma} = \frac{1}{\beta^2\beta'\gamma\gamma'} \left[\sinh x - \frac{\gamma'}{\gamma} x \right]_{x_1}^{x_2}$$

$P_2 = \frac{1}{2}(3 \cos^2\theta^* - 1)$:

$$\frac{a_2^\Lambda}{a_2^\Sigma} = \left|_{\theta_1}^{\theta_2} \cos\theta + \frac{1}{2\beta^3\beta'\gamma\gamma'} \left[\frac{3 \cosh x}{\gamma^2} + 3 \left(\frac{\gamma'^2 + \gamma^2}{\gamma^2} \right) \ln \tanh \frac{1}{2} x - \frac{6\gamma'}{\gamma} \ln(\sinh x) \right]_{x_1}^{x_2} \right.$$

$P_3 = \frac{1}{2}(5 \cos^3\theta^* - 3 \cos\theta^*)$:

$$\frac{a_3^\Lambda}{a_3^\Sigma} = \frac{1}{2\beta^2\beta'\gamma\gamma'} \left[\left(\frac{5}{\beta^2} - 3 \right) \sinh x + \left(\frac{-15\gamma'}{\gamma\beta^2} + \frac{3\gamma'}{\gamma} \right) x - \frac{1}{\sinh x} \left(\frac{5}{\beta^2} \right) \left(1 + 3 \frac{\gamma'^2}{\gamma^2} \right) + \frac{5}{\beta^2} \left(-3 \frac{\gamma'}{\gamma} - \frac{\gamma'^3}{\gamma^3} \right) \left(\frac{\cosh x}{\sinh x} \right) \right]_{x_1}^{x_2}$$

$P_4 = \frac{1}{8}(35 \cos^4\theta^* - 30 \cos^2\theta^* + 3)$:

$$\frac{a_4^\Lambda}{a_4^\Sigma} = \frac{1}{8\beta^3\beta'\gamma\gamma'} \left\{ \frac{-17.5}{\beta^4} \left(1 + \frac{6\gamma'^2}{\gamma^2} + \frac{\gamma'^4}{\gamma^4} \right) \frac{\cosh x}{\sinh^2 x} + \ln \tanh \frac{1}{2} x \right. \\ \times \left[\frac{-17.5\gamma'^2}{\beta^4\gamma^2} \left(-3 - \frac{6\gamma'^2}{\gamma^2} + \frac{\gamma'^4}{\gamma^4} \right) - \frac{30}{\beta^2} \left(1 + \frac{\gamma'^2}{\gamma^2} \right) \right] \\ \left. + \cosh x \left(\frac{35}{\beta^4} - \frac{30}{\beta^2} + 3 \right) + \ln(\sinh x) \frac{\gamma'}{\gamma\beta^2} \left(\frac{-140}{\beta^2} + 60 \right) + \frac{1}{\sinh^2 x} \frac{70\gamma'}{\beta^4\gamma} \left(1 + \frac{\gamma'^2}{\gamma^2} \right) \right\}$$

Decay Parameters in the Nonleptonic Decay Modes of the Charged Σ Hyperons

D. BERLEY AND S. P. YAMIN

Brookhaven National Laboratory, Upton, New York 11973*

AND

S. S. HERTZBACH, R. R. KOFLER, G. W. MEISNER, J. BUTTON-SHAFER, AND S. S. YAMAMOTO

University of Massachusetts,† Amherst, Massachusetts 01002

AND

W. HEINTZELMAN,‡ M. SCHIFF,§ J. THOMPSON, AND W. WILLIS

Yale University,|| New Haven, Connecticut 06520

(Received 2 October 1969)

We present the final results of a measurement of the $\bar{\Sigma}$ decay parameters for $\Sigma^\pm \rightarrow n + \pi^\pm$. We find $\alpha_- = -0.134 \pm 0.034$ and $\alpha_+ = 0.037 \pm 0.049$.¹ Defining ϕ by $\beta = (1 - \alpha^2)^{1/2} \sin\phi$, $\gamma = (1 - \alpha^2)^{1/2} \cos\phi$, we find $\phi_- = (-5 \pm 23)^\circ$ and $\phi_+ = (176 \pm 24)^\circ$.

INTRODUCTION

IN this paper, we present the final results¹ of our measurements of the decay parameters in the decays

$$\Sigma^\pm \rightarrow n + \pi^\pm. \quad (1)$$

* Work performed under the auspices of the U. S. Atomic Energy Commission.

† Work supported in part by the U. S. Atomic Energy Commission, under Contract No. AT(30-1)-3651, and in part by a faculty research grant of the University of Massachusetts.

‡ Present address: Physics Department, Carnegie-Mellon University, Pittsburgh, Pa. 15213.

§ Present address: Laboratoire Leprince-Ringuet, École Polytechnique, Paris, France.

The parameters are defined by

$$\alpha = -2 \operatorname{Re}(s^*p) / (|s|^2 + |p|^2), \quad (2)$$

$$\beta = 2 \operatorname{Im}(s^*p) / (|s|^2 + |p|^2), \quad (3)$$

$$\gamma = (|s|^2 - |p|^2) / (|s|^2 + |p|^2), \quad (4)$$

|| Work supported in part by the U. S. Atomic Energy Commission.

¹ Preliminary results were presented in D. Berley *et al.*, Phys. Rev. Letters **17**, 1071 (1966); **19**, 979 (1967). The value of ϕ_- given in the second of these papers is inconsistent with the convention used therein, though it is consistent with the convention used in this paper.

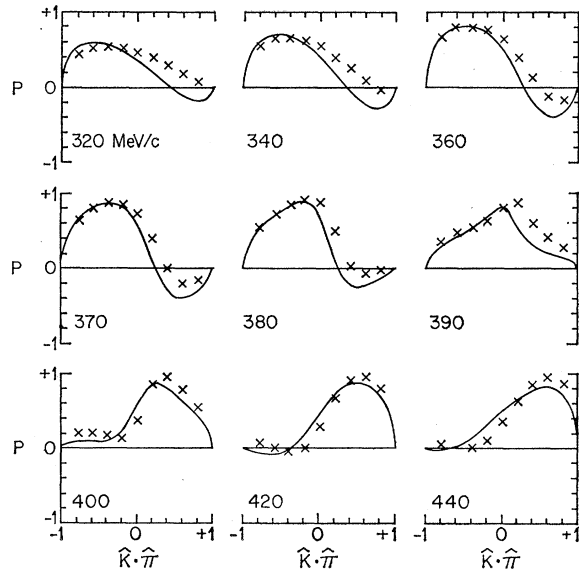


FIG. 1. Polarization of Σ^+ produced by $K^- + p \rightarrow \Sigma^+ + \pi^-$ as a function of $\hat{K} \cdot \hat{\pi}$ for various K^- momenta. \hat{K} and $\hat{\pi}$ are unit vectors in the direction of the K and π momenta in the center-of-mass system.

where s and p are the spin-nonflip and spin-flip amplitudes, respectively. Since α , β , and γ are related by

$$\alpha^2 + \beta^2 + \gamma^2 = 1, \quad (5)$$

we present values for the independent parameters α and ϕ , where

$$\beta = (1 - \alpha^2)^{1/2} \sin \phi, \quad \gamma = (1 - \alpha^2)^{1/2} \cos \phi. \quad (6)$$

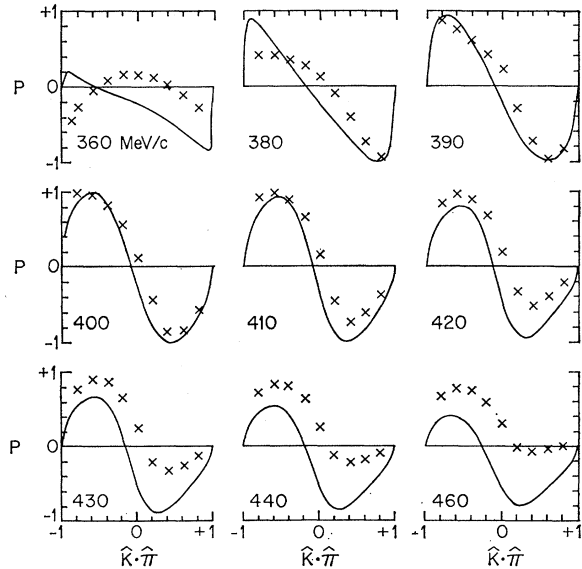


FIG. 2. Polarization of Σ^- produced by $K^- + p \rightarrow \Sigma^- + \pi^+$ as a function of $\hat{K} \cdot \hat{\pi}$ for various K^- momenta. \hat{K} and $\hat{\pi}$ are unit vectors in the direction of the K and π momenta in the center-of-mass system.

The distribution I and polarization \mathbf{P} of the neutrons resulting from the decays (1) are given by

$$I = (1/4\pi)(1 + \alpha \mathbf{P}_\Sigma \cdot \hat{n}), \quad (7)$$

and

$$\mathbf{P} = (1 + \alpha \mathbf{P}_\Sigma \cdot \hat{n})^{-1} \{ (\alpha + \hat{n} \cdot \mathbf{P}_\Sigma) \hat{n} + \beta (\hat{n} \times \mathbf{P}_\Sigma) + \gamma [(\hat{n} \times \mathbf{P}_\Sigma) \times \hat{n}] \}, \quad (8)$$

where \mathbf{P}_Σ is the Σ polarization and \hat{n} is a unit vector in the direction of neutron emission.² The distribution I is measured in the Σ rest frame, and \mathbf{P} is in the neutron rest frame obtained from the Σ rest frame by a Lorentz transformation along \hat{n} . Given a sample of Σ 's of known polarization, the parameter α can be determined from a study of the decay distribution, while a measurement of the neutron polarization is necessary to obtain β and γ (or ϕ).

Watson, Ferro-Luzzi, and Tripp³ (hereafter referred to as WFT) found that the Σ^+ hyperons produced by the reaction

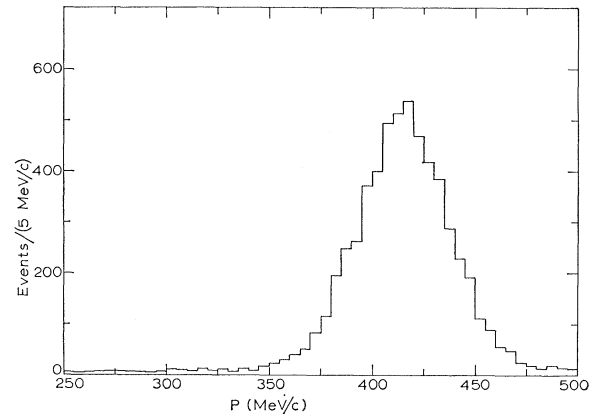
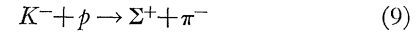
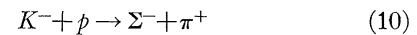


FIG. 3. Beam momentum at production for Σ^- events.

in the vicinity of the $Y_0^*(1520)$ resonance are highly polarized. Their partial-wave analysis predicted that the Σ^- hyperons produced by



are also highly polarized in that energy region.

More recently, Kim has published the results of a multichannel effective-range analysis of the experimental data for the $\bar{K}N$ interaction from 0 to 550 MeV/c.⁴ Figures 1 and 2 show the Σ^+ and Σ^- polariza-

² In this convention, α is equal to the helicity of the nucleon resulting from the decay of an unpolarized Σ . By comparison of Eqs. (7) and (8) with those given in the latest "Review of Particle Properties" [N. Barash-Schmidt, A. Barbaro-Galtieri, L. R. Price, A. H. Rosenfeld, P. Söding, C. G. Wohl, W. Roos, and G. Conforto, Rev. Mod. Phys. 41, 113 (1969)], one notes that the two conventions are related by a change in the sign of β . The value of ϕ must also be changed accordingly.

³ M. Watson, M. Ferro-Luzzi, and R. D. Tripp, Phys. Rev. 131, 2248 (1963).

⁴ J. Kim, Phys. Rev. Letters 19, 1074 (1967).

tions as given by the fits of Kim and WFT⁵ for various beam momenta. The Σ^+ polarizations given by the two fits are in good agreement, as expected. However, there is disagreement for the polarization of backward-produced Σ^- 's above 410 MeV/c. Because the polarization from Kim's fit produces more consistent results for α_- and ϕ_- ,⁶ we have used it in the calculation of the results presented here.

In this experiment, reactions (9) and (10) were utilized to provide sources of polarized Σ 's of both signs. These Σ 's were produced in the 30-in. Columbia-BNL hydrogen bubble chamber, which was exposed to a K^- beam having a momentum of approximately 400 MeV/c. As suggested above, the parameters α_{\pm} were obtained from the decay asymmetries. The parameters ϕ_{\pm} were determined by observing the asymmetry in the neutron-proton scattering in the bubble chamber subsequent to decay.

DATA ACQUISITION

Approximately 1 000 000 bubble-chamber exposures were taken, one-half of them with the beam momentum at production centered at about 375 MeV/c, and one-half at 415 MeV/c (see Figs. 3 and 4). All the film was scanned identically, but only the Σ^+ (Σ^-) events were measured in the lower- (higher-) momentum film.

Scanning was done at Yale and Massachusetts, according to a set of rules designed to minimize the number of background events accepted while maximizing the amount of information available in the events. The lengths quoted in the discussion below are as observed on the Yale scanning tables, which produced projected images having a magnification of approximately 1.1:1.0 when compared to actual spatial distances. Scanning was done primarily in view 2; the other views were used for clarification.

The general topology of an event is shown for a Σ^+ in Fig. 5. In general, the production and decay vertices were required to be at least 5 cm from the nearest edge of the exposure. Track 1, the incident K^- , was required to be a negative track free of visible kinks or scatters.

The production pion, track 2, was required to be at least 1.5 cm long and not aligned with the Σ , track 3. In addition, since backward Σ^+ 's produced at beam momenta less than 375 MeV/c are not strongly polarized, for Σ^+ events the production pion was required to make an angle of at least 130° with the beam track. The Σ was required to be from 1 to 80 mm in length.

⁵ We have used solution I of WFT. The direction of positive Σ polarization is $\hat{K} \times \hat{\pi} / |\hat{K} \times \hat{\pi}|$.

⁶ Using the fit of WFT, we find $\alpha_- = -0.108 \pm 0.038$, $\alpha_+ = 0.035 \pm 0.048$, $\phi_- = -(12 \pm 27)^\circ$, and $\phi_+ = (172 \pm 23)^\circ$. We have also recalculated α_{\pm} and ϕ_{\pm} using the polarization estimates given by a fit done by Thompson. See J. Thompson, thesis, Yale University, 1969 (unpublished). We used the "fit-I" parameters. This fit is essentially the same as that done by Kim, with the addition of data in the $\bar{K}^0 n$, $\Lambda \pi^0$, and $\Sigma^0 \pi^0$ channels. The resulting values are $\alpha_- = -0.120 \pm 0.037$, $\alpha_+ = 0.039 \pm 0.047$, $\phi_- = (-6 \pm 23)^\circ$, and $\phi_+ = (170 \pm 22)^\circ$.

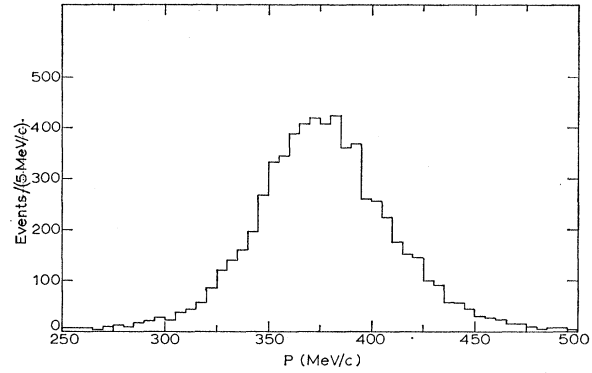


FIG. 4. Beam momentum at production for Σ^+ events.

The maximum length requirement was imposed in order to discriminate against K^-p scatters with a subsequent K^- decay which have a topology similar to Σ^- production and decay.

Track 4, the decay pion, was required to be at least 1.5 cm long and to make an angle of at least 20° with the forward Σ direction. There are two reasons for this angle requirement. First, by not accepting events with a forward decay pion, many events which are actually $\Sigma^+ \rightarrow p + \pi^0$ decays are eliminated. Second, if one has a $\Sigma^\pm \rightarrow n + \pi^\pm$ event with a forward pion, then the neutron will be backward in the center-of-mass system and will have a low laboratory momentum. Low-energy neutrons are not useful because they will not produce recoils of sufficient length, and because the scattering asymmetry is less well known at low energies. For

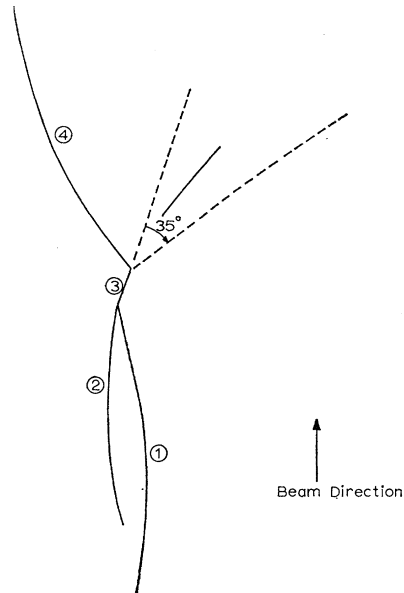


FIG. 5. Topology of a typical Σ^+ event. Track 1 is the incident K^- ; tracks 2 and 3 are the π^- and Σ^+ , respectively; and track 4 is the π^+ resulting from the Σ^+ decay. A possible recoil candidate is shown within the 35° scanning angle.

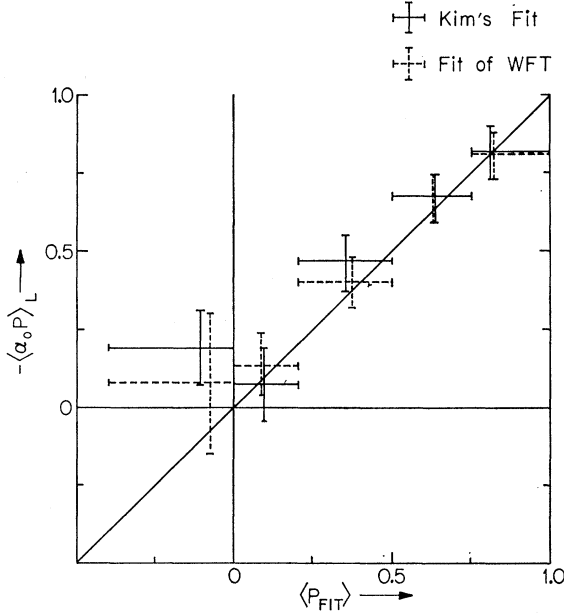


FIG. 6. Decay asymmetry times polarization from $\Sigma^+ \rightarrow p + \pi^0$ decays versus predicted polarization from fits. The horizontal error bars correspond to the sample limits.

further elimination of the $p\pi^0$ decay mode, Σ^+ events were also rejected if track 4 ended in the chamber.

For an event to be accepted, a possible proton recoil had to be visible within 35° of the Σ direction, on the side of the Σ opposite the decay pion. The recoil was required to be a heavily ionizing track at least 5 mm long unless one end was not in the chamber, in which case the length requirement was extended to 5 cm in order that a meaningful momentum measurement could be made from the curvature. The origin of the recoil was defined as the end nearer to the decay vertex. If a recoil lay within the acceptance angle while its origin did not, the recoil was rejected. If the curvature of the track could be determined, it was required to be positive. Lastly, since it was relatively easy to determine if a track originated near the back of the chamber, this criterion was used to eliminate proton tracks entering through the back wall of the chamber. All recoils which passed the above tests were recorded, but only the three nearest the decay vertex were measured.

TABLE I. Fits attempted.

Fit	Reaction	Number of constraints	Unknown variables
1	$K^- + p \rightarrow K^- + p$	3	K^- momentum after scattering
2	$K^- + p \rightarrow \Sigma^\pm + \pi^\mp$	1	Σ momentum and direction
3	$K^- + p \rightarrow \Sigma^\pm + \pi^\mp$	3	Σ momentum
4	$\Sigma^\pm \rightarrow n + \pi^\pm$	1	Neutron momentum and direction
5	$\Sigma^+ \rightarrow p + \pi^0$	1	π^0 momentum and direction
6	$\Sigma^\pm \rightarrow n + \pi^\pm$	3	Neutron momentum
7	$n + p \rightarrow n + p$	1	Neutron momentum and direction after scattering

In addition to the bulk of the events selected as above, approximately 1000 Σ^+ events were selected on the basis of ionization to be probable $\Sigma^+ \rightarrow p + \pi^0$ decays. These events were measured without recoils since the decay asymmetry was the quantity of interest. The ionization selection of these events was done by physicists.

If an event fulfilled all the scanning requirements, a rough sketch was made and other pertinent information was recorded for the measurer.

The bulk of the measurement was done in a three-view three-points-per-track format. The program NP-54 developed at Columbia University was used in the geometrical reconstruction of the particle tracks. The kinematic fitting program used is a modification of HASH, developed at the University of Wisconsin.

Seven fits were attempted. They are listed in Table I. Fit 1 was performed only for events having the topology of Σ^- production and decay. Fits 4-6 were performed only when a successful result had been obtained for either 2 or 3. Similarly, fit 7 was attempted only when fit 6 had been successful.

CLASSIFICATION OF EVENTS

We are interested primarily in three classifications for the Σ^+ events and in two classifications for the Σ^- events. In both cases, we wish to identify the decay modes (1). In addition, we wish to identify Σ decays having an associated neutron-proton scatter. We also want to identify the alternate nonleptonic decay mode $\Sigma^+ \rightarrow p + \pi^0$ for positively charged Σ^+ 's.

In all cases it was required that a satisfactory production fit had been obtained. The criterion used is that the χ^2 for fit 2 must be less than 6 or the χ^2 for fit 3 must be less than 18. In cases in which both production fits were satisfactory, the results of fit 3 were employed in the analysis.

A Σ^- event was accepted as having a satisfactory decay fit if the χ^2 for fit 4 was less than 9. For the Σ^+

TABLE II. Numbers of events in various classifications. Events which are $\Sigma^+ \rightarrow p + \pi^0$ decays are denoted by $\Sigma^+ \rightarrow p$. Events which are $\Sigma^\pm \rightarrow n + \pi^\pm$ decays are denoted by $\Sigma \rightarrow n$. Events having associated recoils are indicated by $n + p$.

	Total	$\Sigma^+ \rightarrow p$	$\Sigma^+ \rightarrow p$ a	$\Sigma \rightarrow n$	$\Sigma \rightarrow n$ a	$\Sigma \rightarrow n$ n + p
Σ^-	7694			6068	5972	1456
Σ^+	7706	1241	1231	4146	4101	1289
		$\Sigma \rightarrow n$ n + p a, b, c	$\Sigma \rightarrow n$ n + p a, b, c, e	$\Sigma \rightarrow n$ n + p a, b, c, f	$\Sigma \rightarrow n$ n + p a, b, c, f	$\Sigma \rightarrow n$ n + p a, b, c, g
Σ^-	1092	29	209	148		706
Σ^+	1054	13	132	185		724

a Beam momentum between 202.5 and 547.5 MeV/c.

b Neutron kinetic energy between 40 and 260 MeV.

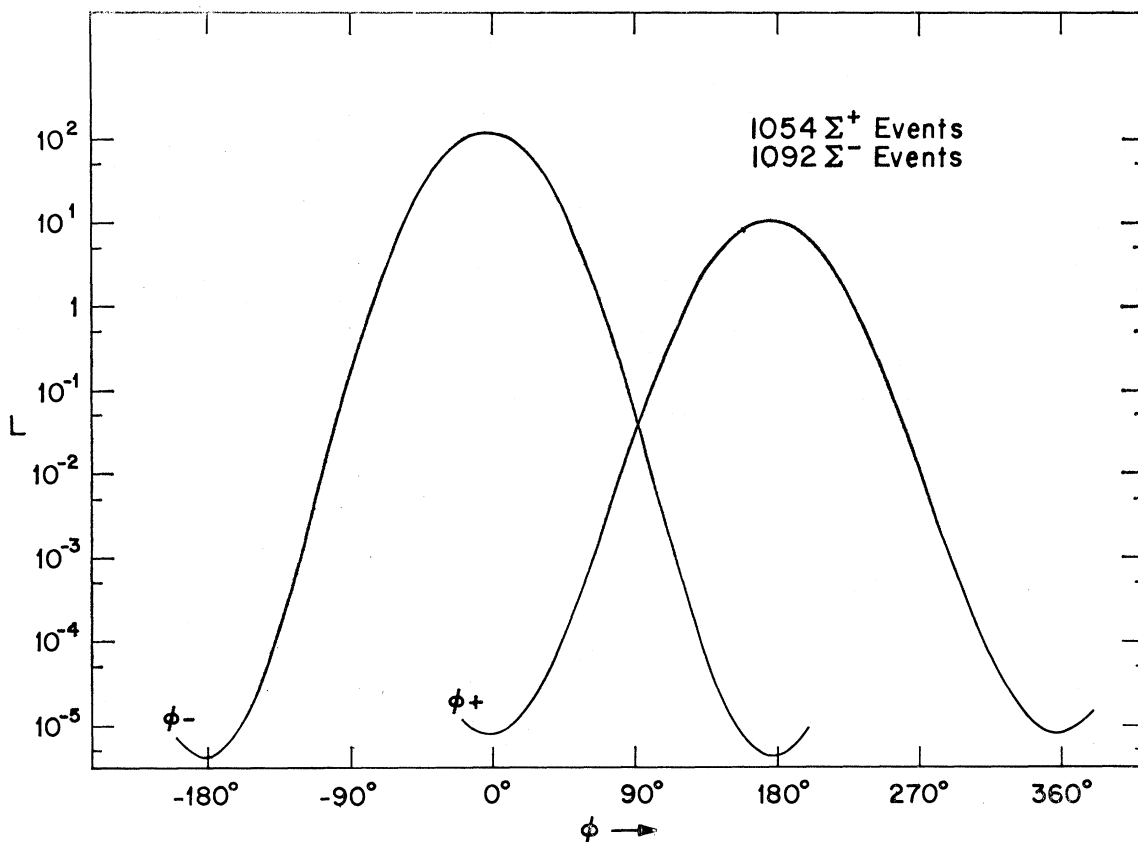
c $\cos\psi > 0.997$.

d $6 < \chi^2(\text{fit } 6) \leq 12$, passes alternate evaluation of scatter.

e $6 < \chi^2(\text{fit } 6) \leq 12$, $\chi^2(\text{fit } 7) \leq 10$.

f $\chi^2(\text{fit } 6) \leq 6$, $\chi^2(\text{fit } 7) > 10$.

g $\chi^2(\text{fit } 6) \leq 6$, $\chi^2(\text{fit } 7) \leq 10$.

FIG. 7. Likelihood functions for ϕ_- and ϕ_+ .

events, an additional complication is introduced by the necessity of separating the neutron and proton decay modes. Three requirements were imposed for a Σ^+ event to be accepted as a decay into the neutron mode. The fit 4 χ^2 had to be less than 9, and the fit 5 χ^2 had to be greater than 50. In addition, the angle between the Σ direction and the charged decay track in the laboratory had to exceed the maximum angle possible for a proton. Events were classified as proton decays if the χ^2 for fit 4 was greater than 9 and that for fit 5 was less than 9. If the χ^2 's for both fits 4 and 5

were less than 9 and the event had been preselected in scanning as a probable $p\pi^0$ event, then the event was classified in the $p\pi^0$ category if the charged decay track ended in the chamber and if its expected range, assuming it to be a proton, was no less than 90% of its measured length. Events remaining ambiguous after this procedure were not used in any subsequent calculations.

The results of fits 6 and 7 are relevant to the selection of associated recoils. Roughly speaking, fit 6 provides an indication of how close the origin of the recoil of

TABLE III. Results of the determination of α_{\pm} .^a

Sample	P_{Kim}	No. of events	$\langle P_{\text{Kim}} \rangle$	$\langle \alpha P \rangle_{\cos\theta}$	$\langle \alpha P \rangle_{\text{up-down}}$	α_L
$\Sigma^+ \rightarrow n\pi^+$						
All events		4101	0.438			0.037 ± 0.049
1	0.0 \rightarrow 0.325	1027	0.155	0.08 ± 0.06	0.10 ± 0.06	0.32 ± 0.28
2	0.325 \rightarrow 0.650	1329	0.502	0.01 ± 0.05	0.05 ± 0.05	0.01 ± 0.09
3	0.650 \rightarrow 1.0	1216	0.766	0.04 ± 0.05	0.03 ± 0.06	0.04 ± 0.06
$\Sigma^- \rightarrow n\pi^-$						
All events		5978	0.581			-0.134 ± 0.034
1	-1 \rightarrow -0.5	2201	0.769	0.12 ± 0.04	0.12 ± 0.04	-0.14 ± 0.05
2	-0.5 \rightarrow 0.0	1280	0.289	0.10 ± 0.05	0.10 ± 0.06	-0.23 ± 0.15
3	0.0 \rightarrow 0.5	1017	0.305	0.02 ± 0.05	0.05 ± 0.06	$+0.09 \pm 0.16$
4	0.5 \rightarrow 1.0	1480	0.743	-0.10 ± 0.04	-0.08 ± 0.05	-0.14 ± 0.06

^a P_{Kim} is the predicted polarization from Kim's fit. The subscripts $\cos\theta$, up-down, and L indicate the method by which the quantity was obtained.

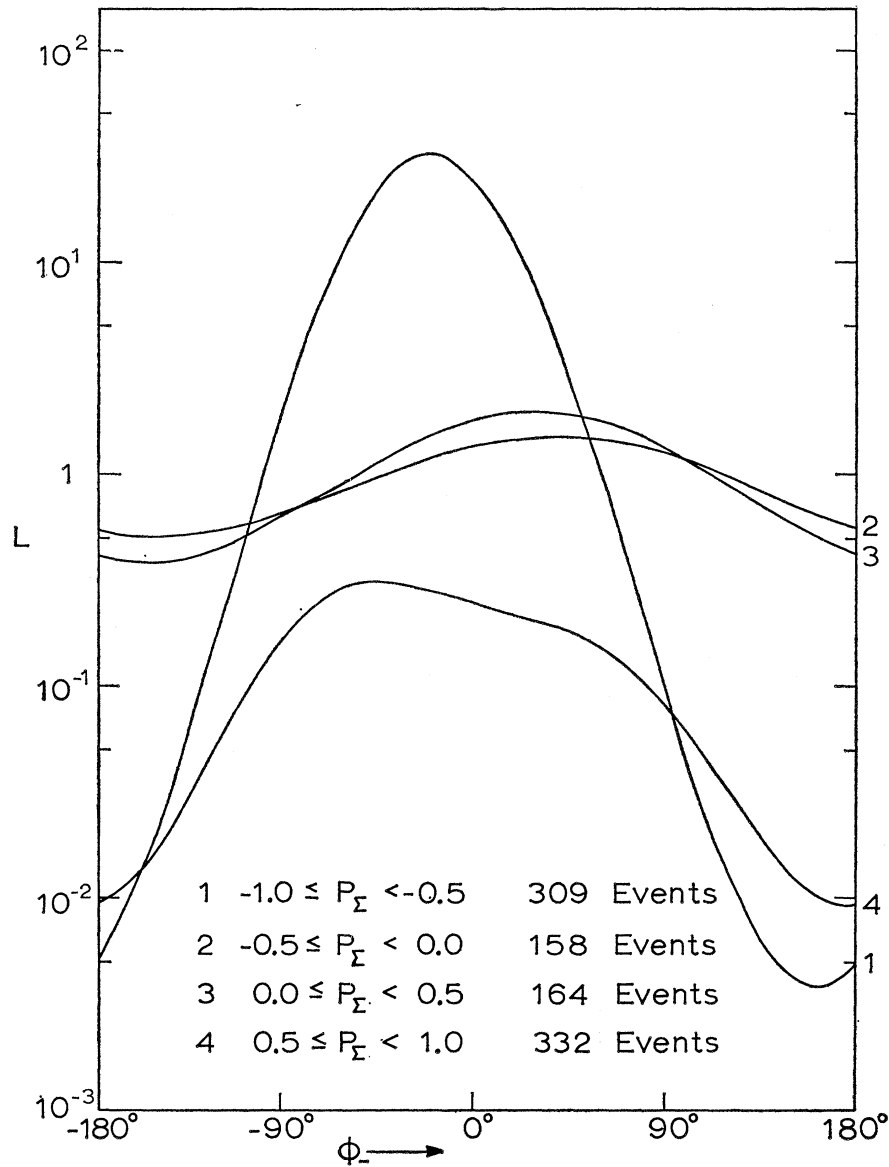


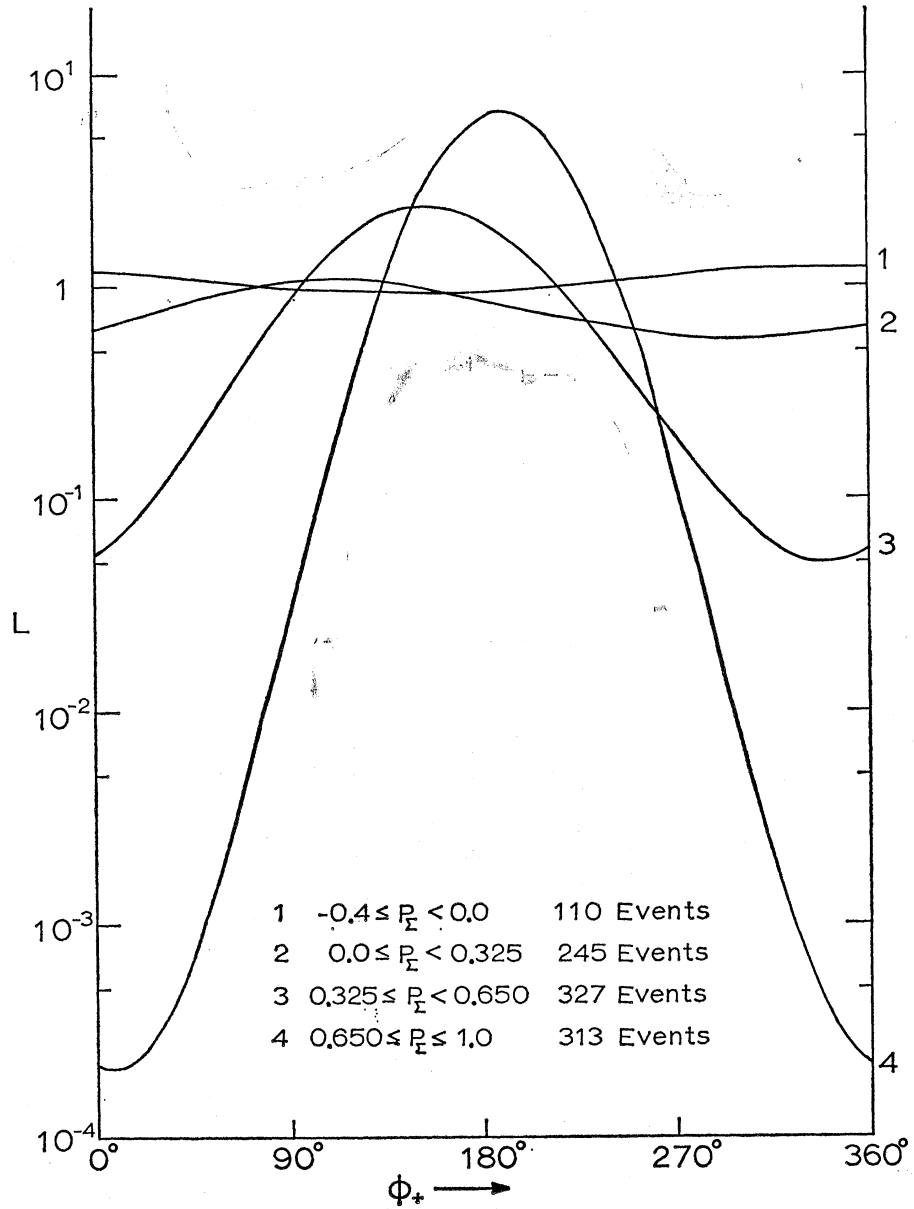
FIG. 8. Likelihood functions for ϕ_- for samples chosen according to the predicted Σ polarization.

interest lies to the line of flight of the neutron. Fit 7 indicates whether the recoil is of the proper momentum to have scattered at the measured angle from a neutron of the momentum obtained from fit 6. Regardless of the results of fit 7, an event was accepted as having a genuine recoil if the χ^2 for fit 6 was less than 6. Events with the χ^2 for fit 6 between 6 and 12 were accepted if the χ^2 for fit 7 was less than 10.

Probably because of difficulties in the fitting routine for very slow, short tracks, there was a large number of events which had a satisfactory fit 6 but failed fit 7 (approximately 180 Σ^- events and 200 Σ^+ events). Another attempt was made to evaluate how well the momentum and direction of a given recoil matched those of the decay neutrons. The momentum of the recoil was calculated from the fitted neutron momen-

tum and direction and the measured recoil direction. This calculation was repeated three times: first, with the inverse of the neutron momentum increased by 1.5%; second, with $\tan\lambda$ and Φ (λ is the dip angle and Φ the azimuthal angle in the chamber coordinate system) of the recoil increased by the amount of their measurement errors; and third, with Φ increased and $\tan\lambda$ decreased. The error in the recoil momentum obtained was taken to be the root mean square of the differences of the latter three values from the first calculated result. This error was combined with the error on the measured momentum of the recoil by taking the square root of the sum of the squares of the two quantities. Let us denote this result by σ_T . Let p_f be the recoil momentum from the above calculation and p_m be the measured recoil momentum. The quantity

FIG. 9. Likelihood functions for ϕ_+ for samples chosen according to the predicted Σ polarization.



given by

$$\delta = |\hat{p}_f - \hat{p}_m| / \sigma_T \tag{11}$$

was used as an alternate evaluation of the scatter. If the χ^2 for fit 6 was between 6 and 12, and δ was less than 2.0, a previously rejected event was accepted as having a genuine recoil. Actually this procedure added relatively few events to the final samples from which ϕ_+ and ϕ_- were calculated. (See Table II.)

Let ψ be the angle between the neutron direction calculated from the 1-C decay fit and the measured neutron direction. After the genuine recoils had been chosen using the criteria discussed above, it was found that there was a small number of so-called "genuine recoils" for which the angle ψ was unreasonably large.

A cut was made at $\cos\psi = 0.997$ ($\psi \approx 4.4^\circ$); all events with $\cos\psi$ less than this value were not used in obtaining the final results.

Also excluded from use in the likelihood function calculations were events having a beam momentum outside of the range 202.5–547.5 MeV/c and events for which the neutron laboratory kinetic energy was less than 40 MeV or greater than 260 MeV.

DETERMINATION OF DECAY ASYMMETRY PARAMETERS

Two customary methods for determining the decay asymmetry parameters employ the relationships

$$\frac{1}{3}\alpha P = \langle \cos\theta \rangle, \tag{12}$$

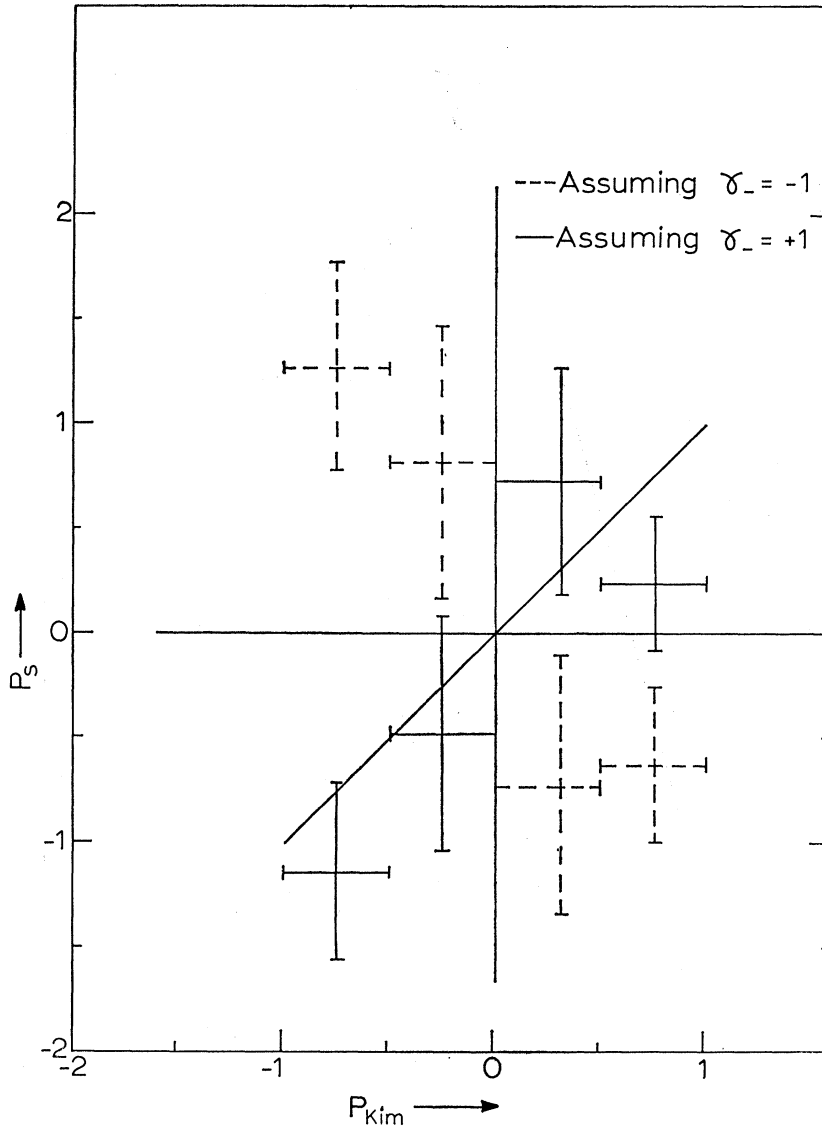


FIG. 10. Σ^- polarization from n - p scattering asymmetry (P_s) versus P_{Kim} , where P_{Kim} is the average predicted polarization for the samples from Kim's fit. The horizontal errors bars correspond to the sample limits.

and

$$\frac{1}{2}\alpha P = (N_{\text{up}} - N_{\text{down}}) / (N_{\text{up}} + N_{\text{down}}); \quad (13)$$

where $\cos\theta = \mathbf{P}_\Sigma \cdot \hat{n} / |\mathbf{P}_\Sigma|$, and N_{up} (N_{down}) is the number of events for which $\cos\theta$ is greater (less) than zero. However, the elimination in scanning of all events for which the angle between the Σ line of flight and the charged decay track is less than 20° can be expected to bias the results obtained from these relationships. On the other hand, the estimation of α by the method of maximum likelihood can be shown to be unbiased by the elimination of events with $|\cos\theta|$ less than some minimum value. Therefore, we have relied primarily upon the method of maximum likelihood to obtain α . The likelihood function

$$L(\alpha) = \prod_{i=1}^N (1 + \alpha P_{\Sigma_i} \cos\theta_i) \quad (14)$$

was calculated, and its maximum was found by interpolation. In Eq. (14), $\cos\theta_i$ is the decay cosine and P_{Σ_i} is* the Σ polarization for the i th event.

It is apparent that a reasonably accurate estimate of the polarization of the Σ produced in a given event is necessary for the success of this experiment. The known large value^{7,8} of the asymmetry in the decay $\Sigma^+ \rightarrow p + \pi^0$ provides a means of checking the accuracy of the fits of WFT and Kim in predicting the Σ^+ polarization.

We have obtained a sample of 1241 decays of this type. Some of these were obtained from a special scan for this decay mode, while the remainder is events eliminated from the $\Sigma^+ \rightarrow n + \pi^+$ sample.

⁷ E. F. Beall, B. Cork, D. Keefe, P. G. Murphy, and W. A. Wenzel, Phys. Rev. Letters **8**, 75 (1962).

⁸ R. O. Bangarter, A. Barbaro-Galtieri, J. P. Berge, J. J. Murray, F. T. Solmitz, M. L. Stevenson, and R. D. Tripp, Phys. Rev. Letters **17**, 495 (1966).

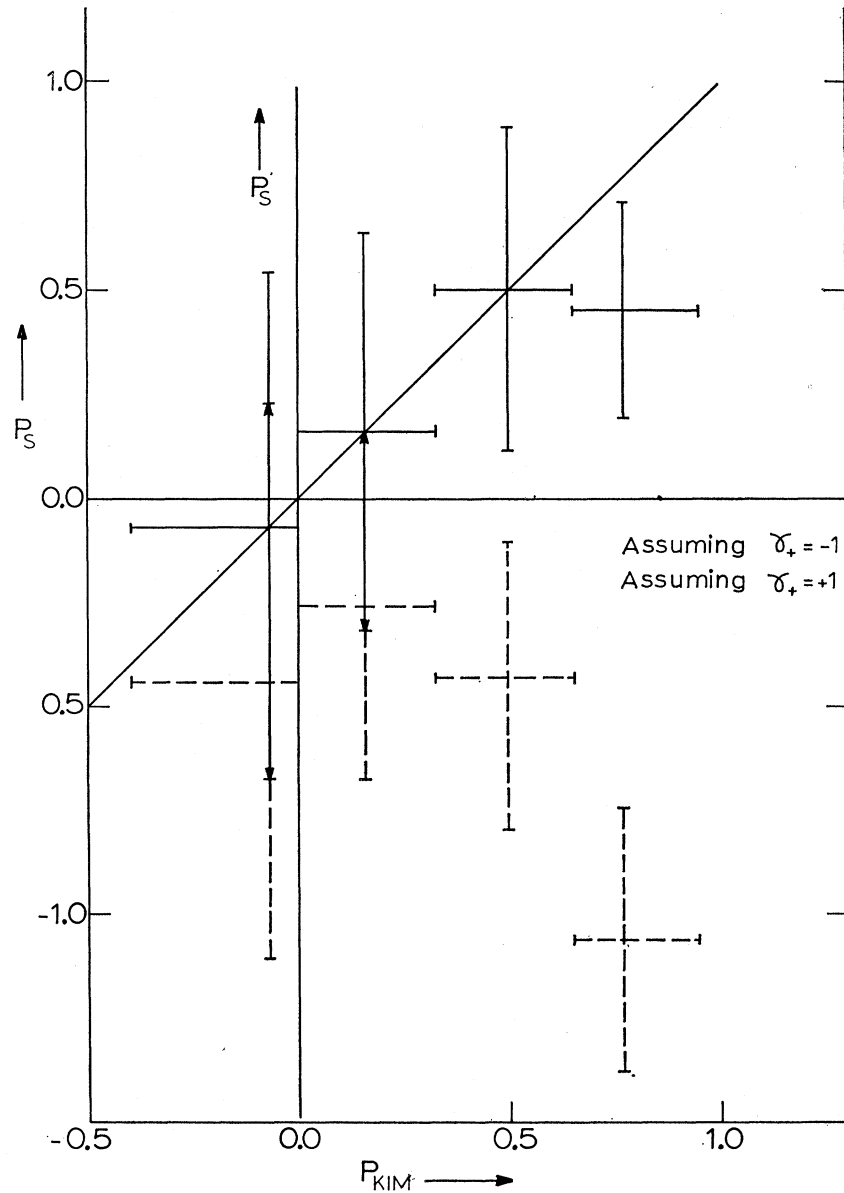


FIG. 11. Σ^+ polarization from n - p scattering asymmetry (P_S) versus P_{Kim} , where P_{Kim} is the average predicted polarization for the samples from Kim's fit. The horizontal error bars correspond to the sample limits.

The events were divided into five subsamples according to the polarization predicted for the events from the fits. The quantity $\alpha_0 P$ was computed for each sample using the method of maximum likelihood. In addition the average predicted polarization was obtained. The results are displayed in Fig. 6. On the vertical axis is plotted the value of $-\alpha_0 P$ along with its uncertainties. The horizontal axis is the average of the predicted polarizations for the events in the sample. The horizontal error bars correspond to the sample limits. The diagonal line drawn on the graph corresponds to the expected locus of the points assuming $\alpha_0 = -1$.

We note that except for the events predicted to have negative polarizations, we have good agreement be-

tween the predicted polarizations and the observed value of $-\alpha_0 P$. Since α_0 is known to be near -1 , we conclude that the analyses of Kim and WFT both provide accurate enough estimates of the Σ^+ polarization.

The results of the analysis for the decay parameters α_+ and α_- are displayed in Table III. In addition to the samples of all events, results are presented for subsamples chosen according to the predicted values of the Σ polarization for the events.

We note that the values of α_- and α_+ lie 3.9 and 0.76 standard deviations from zero, respectively. In addition we see that the Σ^- samples 1 and 4 do give consistent results. This is encouraging in that it agrees with the predicted sign change in the Σ^- polarization.

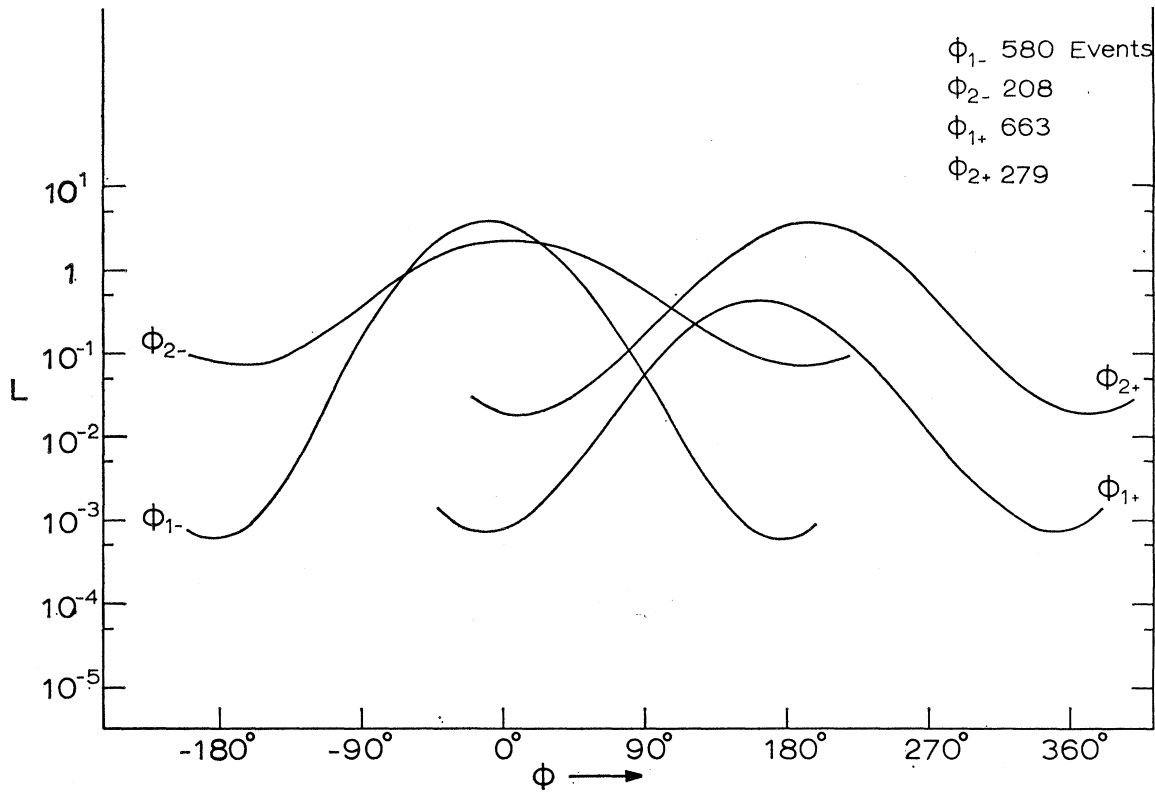


FIG. 12. Likelihood functions for ϕ for events having recoils lying in a restricted volume of the chamber. The numerical subscript indicates the restriction set.

DETERMINATION OF ϕ_- AND ϕ_+

Consider a neutron beam with a polarization \mathbf{P} scattering from an unpolarized proton target. Let \hat{n} and \hat{n}' be the neutron directions before and after scattering, respectively. Define the scattering normal \hat{S} by

$$S = \hat{n} \times \hat{n}' / |\hat{n} \times \hat{n}'|. \quad (15)$$

Let $\chi = \cos^{-1}(\mathbf{P} \cdot \hat{S} / |\mathbf{P}|)$. Then the scatters will have a distribution in χ given by⁹

$$\frac{d\sigma}{d\chi} = \frac{1}{2}(1 + AP \cos\chi) \quad \text{or} \quad \frac{d\sigma}{d\chi} = \frac{1}{2}(1 + A\mathbf{P} \cdot \hat{S}). \quad (16)$$

The quantity A is the scattering asymmetry parameter.¹⁰ It is a function of the neutron energy and of the polar scattering angle, $\cos^{-1}(\hat{n} \cdot \hat{n}')$. For an event with a given Σ polarization and given decay geometry, \mathbf{P} is a function of α and ϕ as indicated in Eqs. (6) and (8).

To obtain the maximum-likelihood estimate of ϕ , we find the maximum of the likelihood function

$$L(\phi) = \prod_{i=1}^N [1 + A_i \mathbf{P}_i(\phi) \cdot \mathbf{S}_i]. \quad (17)$$

⁹ See, e.g., L. Wolfenstein, *Ann. Rev. Nucl. Sci.* **6**, 43 (1956).

¹⁰ The values of the neutron-proton scattering asymmetry parameter A were obtained from tables supplied through the courtesy of G. Breit. The fit from which they were obtained is

Although P is a function of α as well as ϕ , no significant difference was observed in the maximum-likelihood estimate of ϕ for values of α in the range -0.25 to $+0.25$. Therefore, the results presented here were calculated with $\alpha=0$ even though we did find nonzero values for α_+ and α_- from the study of the decay asymmetries.

The actual procedure used to determine ϕ_- and ϕ_+ is as follows. For a given event with an associated recoil, the neutron polarization was obtained from Eq. (8) for 18 values of ϕ from 0° to 340° . These 18 polarization directions were transformed to the scattering vertex taking into account relativistic effects and the precession of the spin direction in the chamber magnetic field. The likelihood function was computed for each of the 18 values of ϕ , and its maximum was found by interpolation.

The likelihood functions obtained for the complete samples of events with associated recoils are presented in Fig. 7. The results are $\phi_- = (-5 \pm 23)^\circ$ and $\phi_+ = (176 \pm 24)^\circ$. Figures 8 and 9 show the likelihood functions for various subsamples, chosen according to the predicted polarizations for the events.¹¹

similar to YLAN3M discussed in M. H. Hull, K. E. Lassila, H. M. Ruppel, F. A. McDonald, and G. Breit, *Phys. Rev.* **122**, 1606 (1961).

¹¹ The samples from which these subsamples were taken are slightly smaller than those from which the values of ϕ_- and ϕ_+ were determined. They contain 969 Σ^- events and 1005 Σ^+ events.

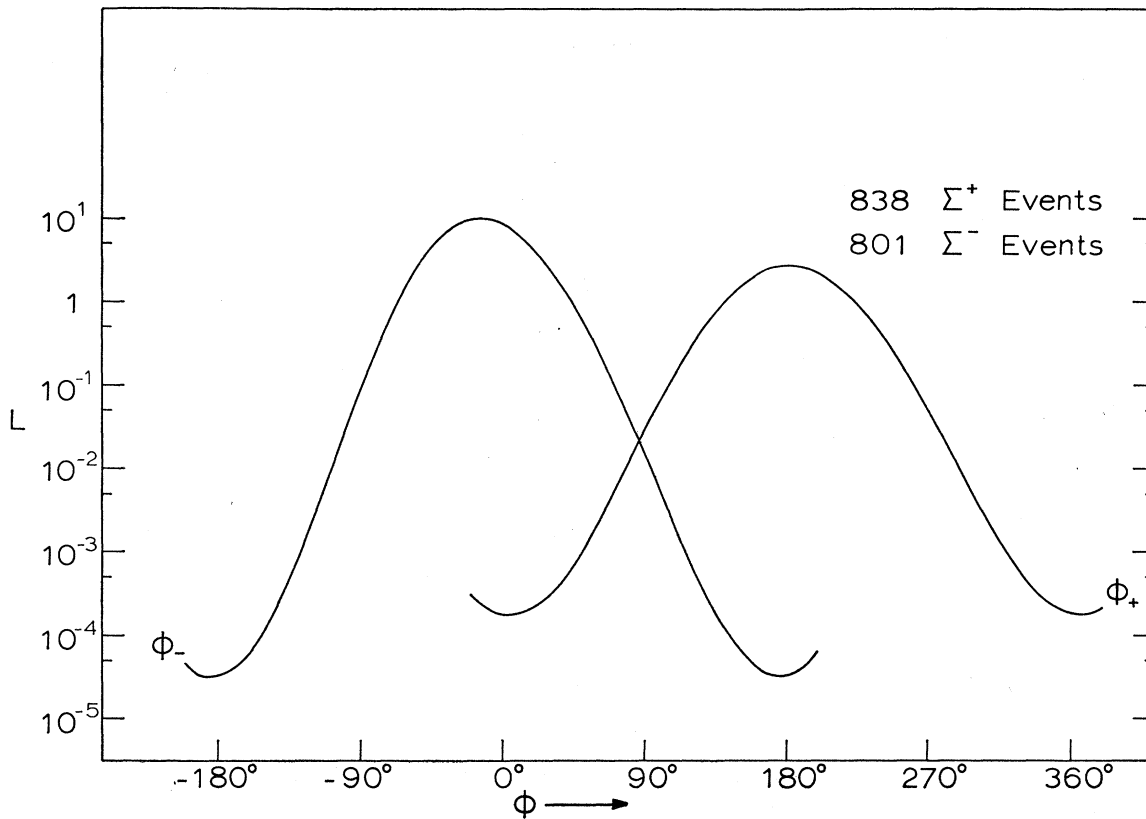


FIG. 13. Likelihood functions for ϕ for events whose recoils have a minimum potential projected length of 1 cm. The potential projected length of a recoil is the smallest projected length it could have if the azimuthal scattering angle were different from the observed value.

In obtaining the results presented above, the Σ polarization was obtained from Kim's fit, and the values of ϕ were determined from the n - p scattering asymmetry. Alternatively, one can assume ϕ and calculate the Σ polarizations. This was done for the same subsamples used above, assuming first $\gamma = -1$ and then $\gamma = +1$. The results are shown in Figs. 10 and 11. The Σ polarizations obtained (again using the method of maximum likelihood) are plotted against the average of the predicted polarizations for the events in the samples. The vertical error bars are the uncertainties in the calculated polarizations, while the horizontal error bars correspond to the sample limits. As expected from the previously mentioned results for ϕ_- and ϕ_+ , these graphs indicate that $\gamma_- = +1$ and $\gamma_+ = -1$ are strongly favored over $\gamma_- = -1$ and $\gamma_+ = +1$. More important, especially for the Σ^- events, is the indication of general consistency between the predicted polarizations and the polarizations calculated with the favored assumptions for the γ 's.

BIASES IN OBTAINING ϕ

In an experiment of this sort one is concerned that an unforeseen scanning or measurement bias might in-

roduce a bias into the final results. For purposes of discussion, let us divide possible sources of bias into two classifications: first, biases introduced by the elimination of some genuine events from the sample; second, biases introduced by the inclusion of background n - p scatters in the sample of events with genuine proton recoils.

It should be apparent that any discrimination against certain geometrical configurations at the Σ production and decay vertices should have no effect on the results of the experiment. Thus an event will make an unbiased contribution to the experimental result if all orientations of the scattering normal are equally observable. That is to say, the contribution of the event is unbiased if other events, identical in every respect except for the orientation of the scattering normal, would not be discriminated against.

The two scanning rules of the greatest importance in selecting or rejecting events for measurement are the angle criterion and the length requirement. It will be recalled that the angle criterion requires the origin of a prospective recoil to lie within 35° (in projection) of the Σ and on the side opposite the decay pion, while the length requirement is a minimum projected length of 0.5 cm for the recoil track. One would be interested in

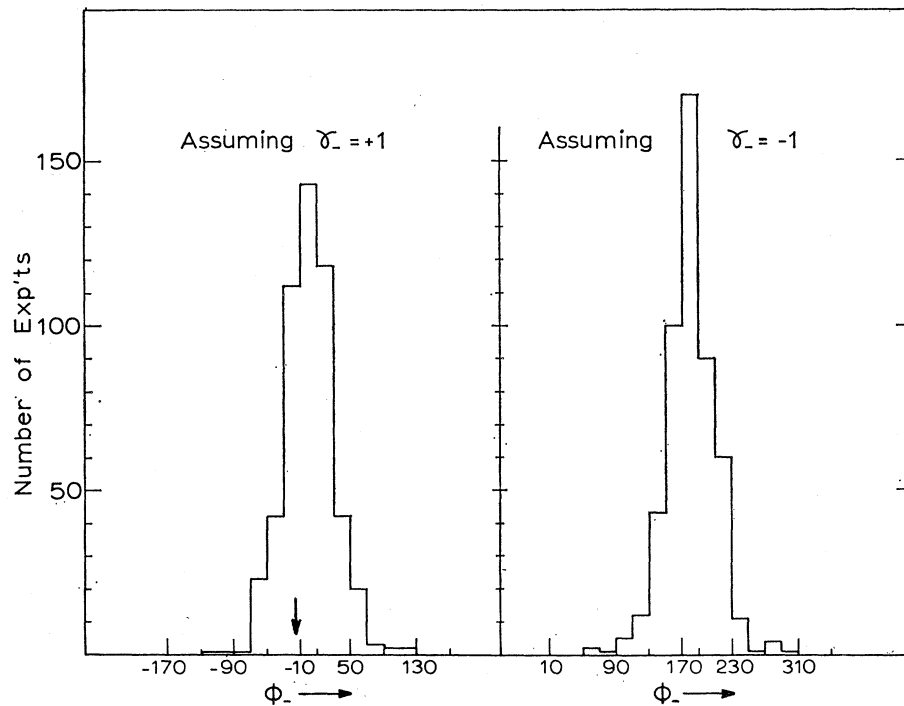


FIG. 14. Σ^- Monte Carlo results—positions of maxima. The arrow indicates the observed value.

showing that these rules have not biased the results. In addition, possible “edge effects” at the physical boundaries of the chamber should be considered.

The possibility of biases due to the limitations of the scanning region can be investigated by making artificial restrictions on the region in which the origin of a recoil lies. For example, one may study a subsample for which all recoil origins lie at least 5 cm from the chamber boundary. Recoils originating near this new boundary should not have biases due to their directional orientation. In Fig. 12 are shown the likelihood functions resulting when recoils with origins outside a given volume are discarded. Three restrictions are imposed. These are limits on the z coordinate, on r , the distance of the recoil from the symmetry axis of the chamber, and on the allowed scanning angle ω_s , which is the projected angle between the Σ direction and the Σ -decay-vertex-recoil-origin line. Shown are the results for two different sets of restrictions:

Set 1	Set 2
$5 \leq z \leq 29$ cm	$10 \leq z \leq 24$ cm
$r \leq 25$ cm	$r \leq 20$ cm
$5^\circ \leq \omega_s \leq 30^\circ$	$10^\circ \leq \omega_s \leq 25^\circ$

The events remaining after removal of recoils lying outside these limits still favor $\gamma_- = +1$ and $\gamma_+ = -1$, though the errors have increased because of the reduced numbers of events.

A similar calculation was done to ensure that the minimum-recoil-length requirement did not introduce

a bias. For a given polar scattering angle, some orientations of the scattering normal might be rejected because the projected recoil length would be too short. Therefore, the recoil direction for a given event was allowed to precess around the initial neutron direction, keeping the polar scattering angle constant. The angle giving the minimum projected length as observed in view 2 was found and that minimum length was calculated. If the minimum projected length was less than a specified value, the event was eliminated from the sample. Figure 13 shows the likelihood functions for a cutoff of 1.0 cm. After the elimination of events which are a possible source of bias, we still find essentially the same results.

MONTE CARLO CALCULATIONS

A series of Monte Carlo calculations was made, primarily to determine how probable it is for one to obtain the observed results when the physical values of γ_\pm are opposite in sign to those observed.

The measured events used in the determination of ϕ_- and ϕ_+ were used as the basis for these calculations. A certain value of ϕ was assumed to be the true physical value. To each event was assigned a new random direction for the scattering normal, perpendicular to the neutron line of flight, and chosen in such a way that if ν is equal to $\cos^{-1}(\hat{P} \cdot \hat{S})$, then the distribution of the scattering normals is of the form

$$\frac{dN}{d\nu} \propto 1 + AP \cos \nu. \quad (18)$$

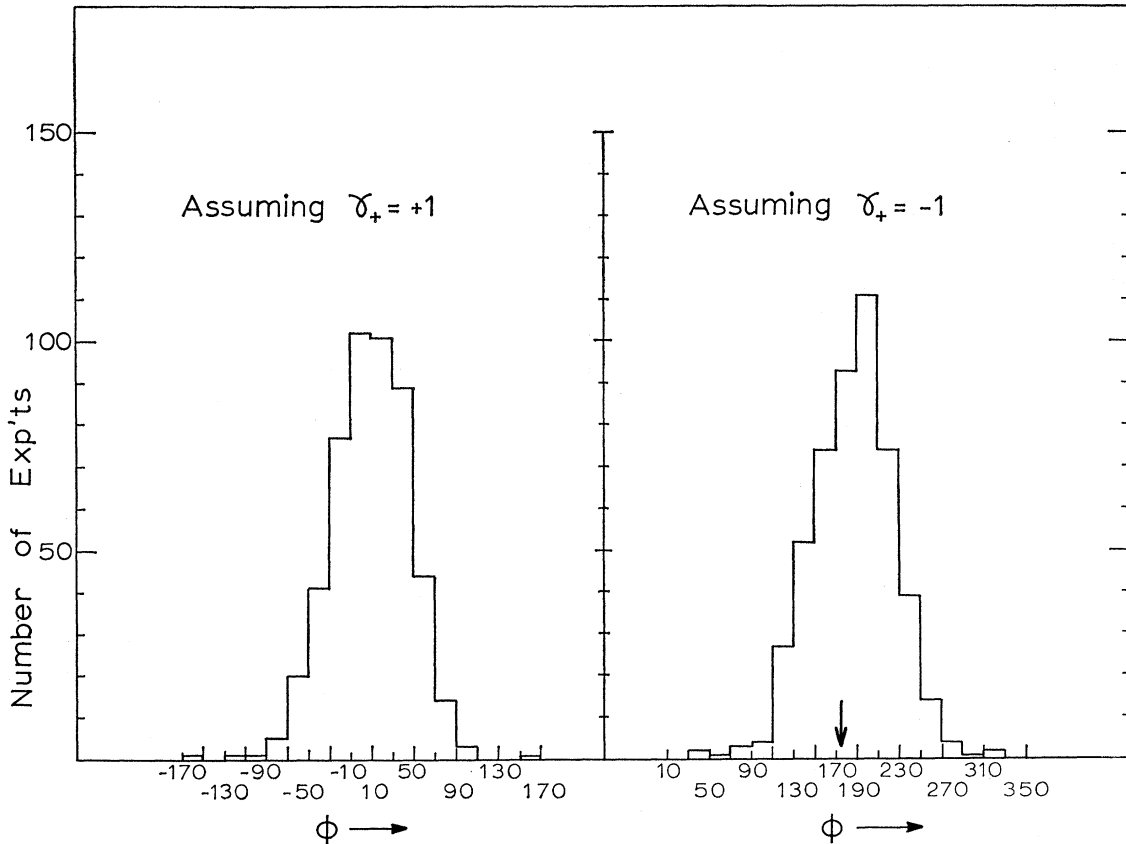


FIG. 15. Σ^+ Monte Carlo results—positions of maxima. The arrow indicates the observed value.

Here \hat{S} is the direction of the assigned scattering normal, \mathbf{P} is the transverse nucleon polarization at the scattering vertex for the assumed value of ϕ , and A is the scattering asymmetry parameter from the measured event.

After a new scattering normal had been assigned, a maximum-likelihood calculation was carried out in exactly the same way as for the measured recoils. In each of the cases to be discussed, 500 experiments were simulated in this way. Four runs were made, first assuming $\phi=0^\circ$ ($\gamma=+1$) and then $\phi=180^\circ$ ($\gamma=-1$), for both the Σ^- and Σ^+ events.

In Fig. 14 are histograms of the positions of the maxima of the resulting Σ^- likelihood functions for the two assumptions for γ_- . The corresponding histograms for the Σ^+ events are shown in Fig. 15. When the value of γ opposite in sign to that actually observed is assumed, for neither charge does one find any of the 500 Monte Carlo experiments producing a value of ϕ in the same bin as that observed. Therefore, the chances of finding the observed results ($\gamma_\pm \sim \mp 1$) when $\gamma_\pm = \pm 1$ are the real values are less than 1 in 500.

However, the strength of the above reasoning is dependent upon how well the Monte Carlo experiments simulate the actual experiment. In Figs. 16 and 17 are shown the distributions of the logarithms of the maxi-

imum values of the likelihood functions and of the likelihood ratios assuming $\gamma_- = +1$ and $\gamma_+ = -1$. For the Σ^- events the observed maximum value of L is about 17, and the likelihood ratio of the maximum and minimum values is 1.7×10^6 . Both these values fall near the peaks of the Monte Carlo results, indicating a good degree of agreement. For the Σ^+ events the corresponding values are 10 and 1.0×10^6 . While the maximum value is again near the peak of the Monte Carlo distribution, the likelihood ratio is higher than expected though still within the Monte Carlo distribution.

STUDIES OF BACKGROUND EVENTS

It is important to know whether the background events favor a particular value of ϕ primarily so that one would know what to expect if some of those events were incorrectly classified as genuine events.

Because the background recoils were not produced by the neutron resulting from the decay of the Σ under consideration, it is necessary to take some freedom with the measurements if one wishes to calculate a value of ϕ for the background events. In order to make this calculation, the origin of the measured recoil was translated to the calculated line of flight of the neutron. The distance of the recoil from the decay vertex was kept

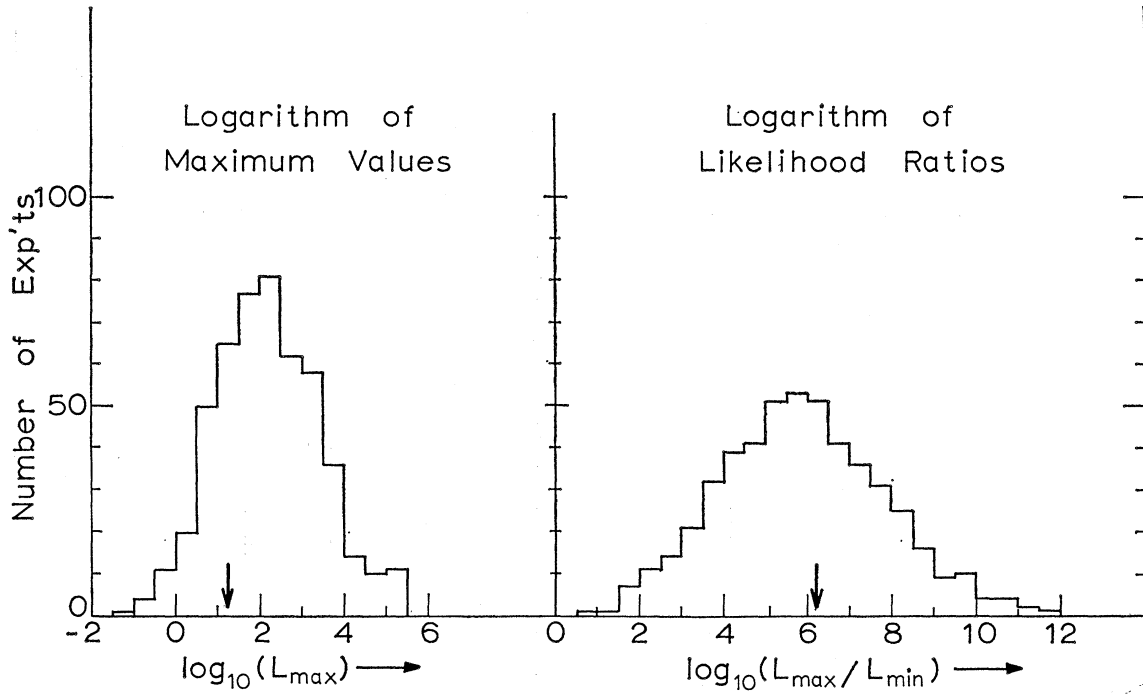


FIG. 16. Σ^- Monte Carlo results with $\gamma_- = +1$ assumed. The arrows indicate the observed values.

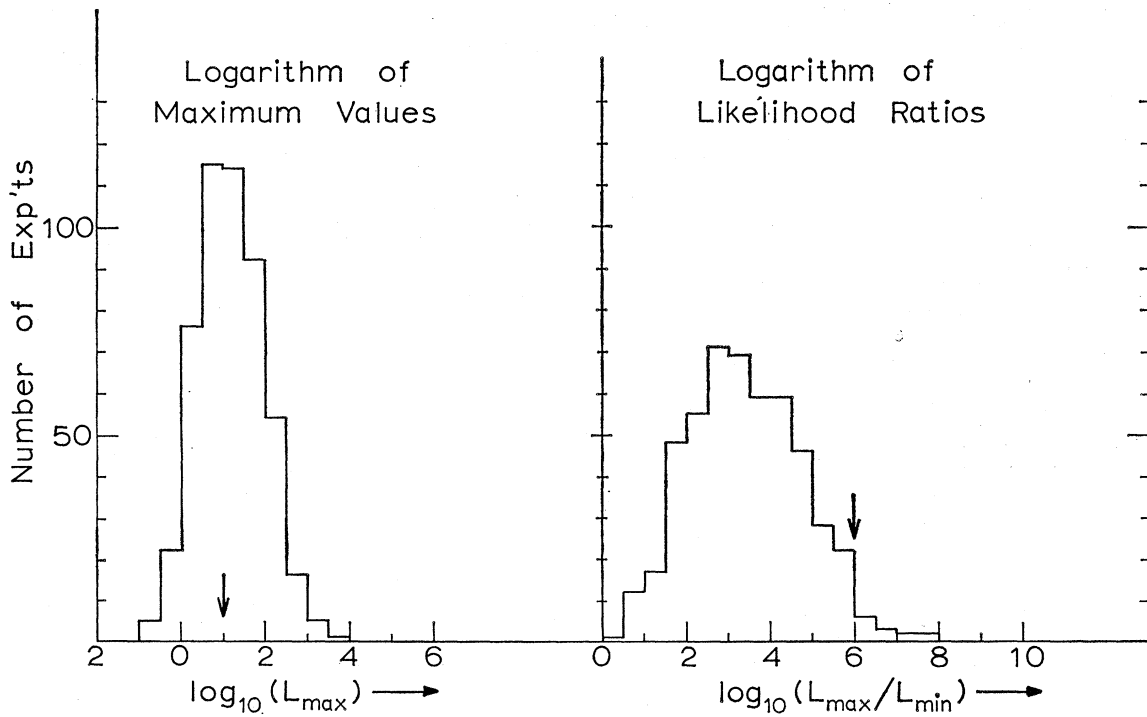


FIG. 17. Σ^+ Monte Carlo results with $\gamma_+ = -1$ assumed. The arrows indicate the observed values.

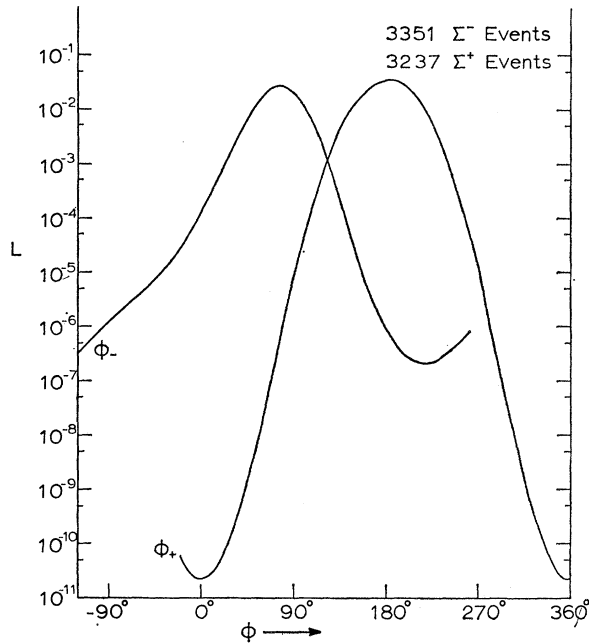


FIG. 18. Likelihood functions for ϕ_{\pm} for complete background samples.

constant and the directional orientation of the recoil was maintained. Then one can compute the scattering angle for the event, determine the appropriate value for the scattering asymmetry, and make a calculation identical to that done for the genuine events. In making this calculation, all information concerning the magnitude of the recoil momentum was ignored.

In Fig. 18 are shown the likelihood functions resulting. For the Σ^- events, there is peaking near 80° , while for the Σ^+ background there is peaking near 180° . One is especially concerned about the Σ^+ result since it indicates that contamination by background could produce the same result as observed from the sample of genuine recoils.

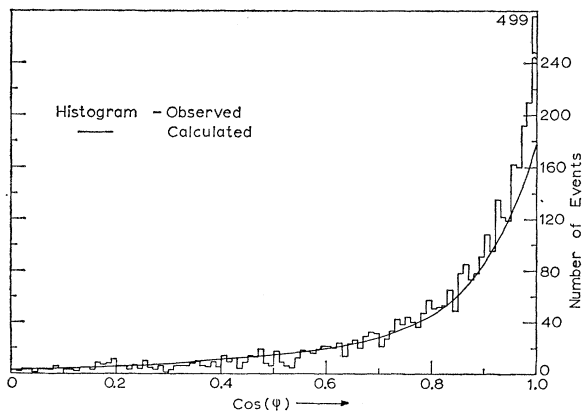


FIG. 19. $\text{Cos}\psi$ distribution for the Σ^- background, where ψ is the angle between the measured neutron direction and the direction calculated from the 1-C decay fit.

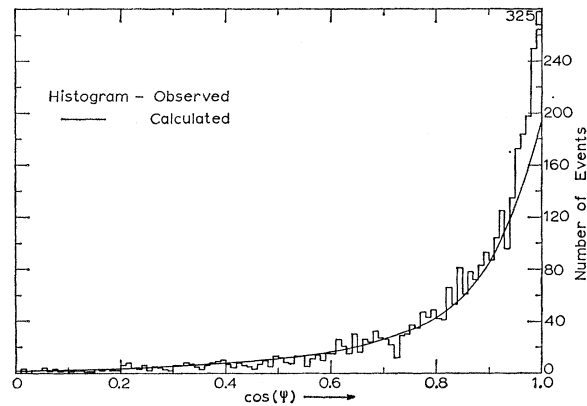


FIG. 20. $\text{Cos}\psi$ distribution for the Σ^+ background, where ψ is the angle between the measured neutron direction and the direction calculated from the 1-C decay fit.

Let ψ be the angle between the neutron direction calculated from the 1-C decay fit and the measured neutron direction. Assuming a uniform distribution of the recoil positions in the chamber, if there were no scanning restrictions (e.g., the 35° rule) and if the decays occurred in the center of a spherical chamber, one would expect the distribution of the background recoils to be uniform in $\text{cos}\psi$. However, this is far from true; the observed distributions are shown in Figs. 19 and 20.

A calculation was made to determine the form of the expected distribution. In this calculation a uniform spatial distribution of recoils within the bubble chamber was assumed. The chamber was taken to be cylindrical with a radius of 30 cm and a depth of 33 cm. The chamber boundaries and the 35° scanning angle rule

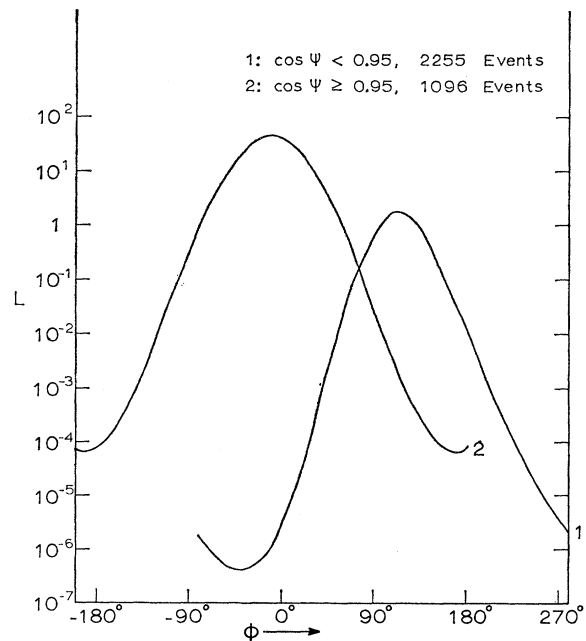


FIG. 21. Likelihood functions for subsamples of the Σ^- background.

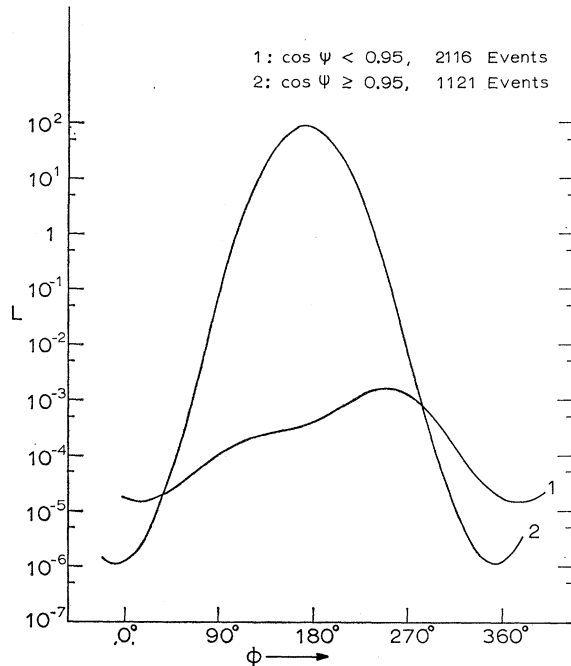


FIG. 22. Likelihood functions for subsamples of the Σ^+ background.

impose limitations on the volume in which a recoil can lie and still be accepted for measurement. Let us call this volume the scanning volume; a recoil lying inside the scanning volume will be measured, while one lying outside is ignored. A numerical integration was done over the scanning volume for constant values of $\cos\psi$, and the contributions from the individual background events were added together to obtain the over-all expected distribution. The distribution was normalized to the observed distribution between $\cos\psi=0.5$ and $\cos\psi=0.9$, using a χ^2 minimization procedure. This is a one-parameter fit since only a normalizing constant is undetermined. The measured background recoils were histogrammed into 40 bins in this range of $\cos\psi$, so

there are 39 constraints. The χ^2 's obtained for the fits are 84.4 for the Σ^+ background and 55.3 for the Σ^- background. The continuous lines drawn on Figs. 19 and 20 are the normalized expected distributions. Note that the observed peak at $\cos\psi=1$ is much larger than expected, while the remainder of the distribution agrees reasonably well with the calculation.

After the peaks in the $\cos\psi$ distributions had been observed, it was decided to make likelihood-function calculations for subsamples of the background chosen according to the value of $\cos\psi$. The results are shown in Figs. 21 and 22 for a division at $\cos\psi=0.95$. We see that the events with $\cos\psi \geq 0.95$ for both the Σ^- and Σ^+ background strongly favor the values of ϕ actually observed from the good events. Considering the change in the value of ϕ with the change in the sign of the Σ , together with the fact that this occurs for the events with $\cos\psi \geq 0.95$, it is reasonable to conclude that the anomalous peaks in the $\cos\psi$ distributions are produced by genuine scatters which failed to make a good fit.

One can estimate from the fitted background curves the number of background events with $\cos\psi > 0.997$. Comparing this number with the number of accepted genuine events gives an estimate of $\leq 5\%$ background contamination in the accepted events. This amount is too small to have a significant effect on the result.

ACKNOWLEDGMENTS

We wish to thank the many people involved with this experiment for their individual contributions. The support of the Brookhaven bubble-chamber group, the alternating-gradient synchrotron staff, and the beam-separator group was essential, as were the efforts of the Yale and Massachusetts scanning and measuring personnel. We are specifically indebted to Professor G. Breit for providing tables of $n-p$ scattering asymmetries. We would also like to thank the rest of the high-energy physics group at Yale for their help and cooperation.